The Journal of Chemical Physics

Definitive *ab initio* structure for the $\tilde{X}\,^2\acute{A}H_2PO$ radical and resolution of the P–O stretching mode assignment

Cite as: J. Chem. Phys. **109**, 2694 (1998); https://doi.org/10.1063/1.476869
Submitted: 23 March 1998 . Accepted: 08 May 1998 . Published Online: 04 August 1998

Steven S. Wesolowski, Eric M. Johnson, Matthew L. Leininger, T. Daniel Crawford, and Henry F. Schaefer

View Online Export Citation

ARTICLES YOU MAY BE INTERESTED IN

In search of definitive signatures of the elusive NCCO radical
The Journal of Chemical Physics **127**, 014306 (2007); https://doi.org/10.1063/1.2747241

Challenge us.
What are your needs for periodic signal detection?
Zurich Instruments
Watch

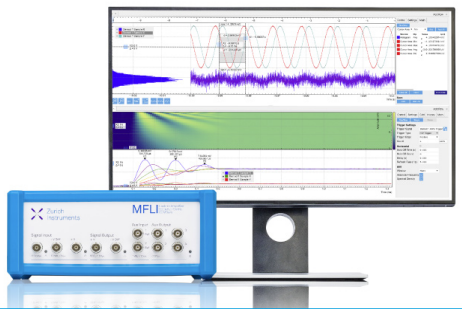

© 1998 American Institute of Physics.

Definitive *ab initio* structure for the $\tilde{X}\,^2A'$ H_2PO radical and resolution of the P–O stretching mode assignment

Steven S. Wesolowski, Eric M. Johnson, Matthew L. Leininger, T. Daniel Crawford, and Henry F. Schaefer III
Center for Computational Quantum Chemistry, University of Georgia, Athens, Georgia 30602-2525

(Received 23 March 1998; accepted 8 May 1998)

Previous *ab initio* studies of the $\tilde{X}\,^2A'$ H_2PO radical have reported dramatically differing P–O bond distances when using spin-restricted wave functions predicting two artifactual isomers of H_2PO: a singly bonded oxygen-centered radical and a doubly bonded phosphorus-centered radical. We show that large basis sets coupled with high levels of dynamical electron correlation are required to correctly describe the P–O bond in H_2PO as well as the unpaired electron density as evidenced by the Fermi contact terms and anisotropic components of the ^{31}P, ^{1}H, and ^{17}O hyperfine splitting (hfs) constants. The optimized geometry, harmonic vibrational frequencies, and hfs constants of H_2PO were determined at several coupled-cluster levels of theory using both spin-restricted (ROHF) and spin-unrestricted (UHF) Hartree–Fock reference wave functions. The geometrical parameters at the coupled-cluster level with single, double, and perturbatively applied triple substitutions [CCSD(T)] using Dunning's correlation consistent polarized valence quadruple-ζ basis set (cc-pVQZ) are $r(\mathrm{P–O}) = 1.492$ Å; $r(\mathrm{P–H}) = 1.410$ Å; $\angle(\mathrm{HPH}) = 102.63°$; $\angle(\mathrm{HPO}) = 114.92°$. These are in excellent agreement with those derived from recent gas phase microwave data, with the surprising exception of the P–H distance which deviates 0.02 Å from experiment. The value of the P–O harmonic stretching frequency at the CCSD(T) level within the cc-pVQZ basis set is 1190 cm^{-1}, in good agreement with the experimental fundamental frequency of 1147 cm^{-1} obtained by Withnall and Andrews and in constrast to previous speculation that this experimental band may have been misassigned. Hyperfine splitting constants determined at the TZ2P(f,d)/UHF-CCSD(T) level are in very good agreement with experimental values with an average deviation of 23 MHz. © *1998 American Institute of Physics.* [S0021-9606(98)30131-2]

I. INTRODUCTION

Phosphoryl radicals (also known as phosphinoyl, phosphonyl, phosphinyl, or phosphono radicals) of the general formula R_1R_2PO are used in a number of industrial polymerization processes.[1–3] The ultraviolet irradiation of various acylphosphine oxides results in cleavage of the P–C(O)R′ bond yielding an aroyl-phosphoryl radical pair, and the high reactivity of phosphoryl radicals toward a myriad of olefinic compounds[4–7] makes them particularly effective initiators of free radical reactions. One of the most useful polymerization reactions involves the α cleavage of mono- and bisacylphosphine oxides which begins the formation of polymer coatings. The subsequent reactions of these diphenylphosphoryl-aroyl pairs are unique in that the yellow hue typically developed during the curing process gradually disappears, making them ideal for white lacquer applications.[3] Since the unpaired electron of phosphoryl radicals may delocalize over both the phosphorus and oxygen atoms to varying degrees, the spin density distribution also plays a key role in predicting the likely structures of radical recombination products and their relative rates of formation.[5,8]

The dihydrophosphoryl radical, H_2PO (Fig. 1) serves as a model compound for alkyl and aryl disubstituted phosphoryls involved in industrial polymers and also illustrates several potential caveats associated with *ab initio* descriptions of the phosphoryl bond. The oxidation of phosphine (PH_3) yields many phosphorus-bearing intermediates, some of which have only recently been observed spectroscopically in the gas phase. Among these, H_2PO has been produced by Hirao, Saito, and Ozeki[9] using a dc glow discharge in a mixture of PH_3 and CO_2 and subsequently identified and precisely characterized by microwave spectroscopy. In previous experimental studies[8,10–14] various aliphatic and aromatic organic derivatives of H_2PO have been produced in solid or solution by photolysis, followed generally by electron spin resonance spectroscopy (ESR).[10] This technique, coupled with the microwave analysis of Hirao and coworkers, has provided information concerning the molecular geometry of H_2PO and the hyperfine splitting constants of closely related radicals. In addition, the vibrational analysis of H_2PO in an Ar matrix has been performed by Withnall and Andrews,[15] yielding results which have disagreed with certain theoretical predictions. Of particular interest is the discrepancy in the frequency of the mode assigned to the P–O stretch which Withnall and Andrews identified at 1147 cm^{-1}. Theoretical predictions for this frequency using spin-unrestricted Hartree–Fock methods (UHF), however, have been approximately half that value ($\sim$600 cm^{-1}).[16,17]

Although possible misassignment of the band at 1147 cm^{-1} has been suggested,[16] a fascinating possible explanation has been offered by deWaal, Aagaard, and Janssen.[10] These authors demonstrated that spin-restricted

 © 1998 American Institute of Physics

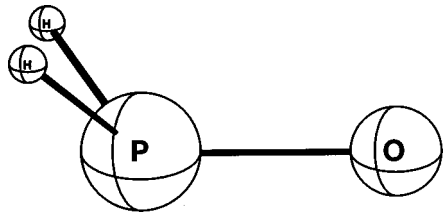

FIG. 1. The C_s structure of the H_2PO radical.

open-shell Hartree–Fock (ROHF) energies calculated over a range of fixed P–O bond lengths within a 6-31G* basis reveal two separate minima corresponding to two resonance structures for H_2PO: an oxygen-centered radical at $r(\mathrm{P–O}) = 1.616$ Å and a zwitterionic phosphorus-centered radical at $r(\mathrm{P–O}) = 1.471$ Å. Geometry optimizations using UHF wave functions on the other hand produced only one minimum at $r(\mathrm{P–O}) = 1.589$ Å, but this bond length is *shortened* considerably to 1.495 Å at the second-order Møller–Plesset perturbation theory (UMP2) level in opposition to expected trends.[16]

In contrast to the localized ROHF description of the unpaired electron, experimentally derived spin distributions suggest the unpaired electron to be highly delocalized primarily between the phosphorus and oxygen atoms but with an unusually high density on the hydrogens as well.[9] Despite the lack of a consensus concerning the molecular geometry of H_2PO, there have been a number of *ab initio* studies investigating the hyperfine splitting constants of this radical.[10,16–18] DeWaal, Aagaard, and Janssen[10] first determined isotropic hyperfine couplings (i.e., Fermi contact terms, a_F) in their study, finding $a_F(^{31}\mathrm{P})$ constants of 135 and 942 MHz for the long and short 6-31G*/ROHF energy minima, respectively. These authors concluded that an accurate prediction of the P–O bond length is essential for a correct spin density distribution. Since then Hirao and co-workers[9] have provided the first experimentally determined $a_F(^{31}\mathrm{P})$ of 1023.43 MHz. However, theoretical predictions of the Fermi contact term for ^{31}P have often struggled to reach even qualitative agreement with this value.[10,16–18]

Clearly, the predicted structure and properties of H_2PO greatly depend on the level of theory employed. Previous theoretical work has been limited to geometries optimized at the UHF, ROHF, and UMP2 levels of theory and have yielded widely scattered results.[10,16,17,19–21] In an effort to elucidate the true structure, vibrational assignments, and hyperfine splittings, we have carried out a high-level *ab initio* investigation of the H_2PO radical.

II. THEORETICAL METHODS

Three basis sets were employed in this study. The smallest was a double-ζ plus polarization (DZP) basis consisting of the standard Huzinaga–Dunning–Hay[22–24] set of contracted Gaussian functions and sets of five *d*-type and three *p*-type polarization functions from Dunning's correlation-consistent double-ζ (cc-pVDZ) basis sets[25,26] added to the heavy atoms and hydrogen atoms, respectively. The contraction scheme for the double-zeta portion of this basis set was P$(12s8p/6s4p)$, O$(9s5p/4s2p)$, H$(4s/2s)$. A TZ2P(f,d) basis was formed with the McLean–Chandler[27] (P atom) and Huzinaga–Dunning[22,28] (O and H atoms) sp sets augmented with two sets of polarization functions from Dunning's cc-pVTZ sets[25,26] (two sets of five *d*-type functions on P and O and two sets of *p* functions on H) as well as a set of seven *f*-type functions[29] on P and O and a set of five *d*-type functions[30] on H. The contraction scheme for the triple-ζ portion of this basis set was P$(13s10p/6s5p)$, O$(11s5p/6s3p)$, H$(5s/3s)$. The largest basis set used was the full cc-pVQZ basis set of Dunning[25,26] with a contraction scheme of P$(16s11p3d2f1g/6s5p3d2f1g)$, O$(12s6p3d2f1g/5s4p3d2f1g)$, H$(6s3p2d1f/4s3p2d1f)$. The DZP basis set contained 48 total basis functions while the TZ2P(f,d) and cc-pVQZ basis sets contained 97 and 174 functions, respectively.

Energies were obtained using both ROHF and UHF wave functions as well as singles and doubles coupled-cluster (CCSD),[31,32] and CCSD including perturbatively applied connected triple excitations [CCSD(T)].[33–35] Both UHF and ROHF references were used with the CCSD and CCSD(T) methods. No orbitals were frozen in the correlated calculations. The ground state $^2A'$ occupation of the H_2PO radical's molecular orbitals in C_s symmetry is

$$[\mathrm{core}](6a')^2(7a')^2(8a')^2(2a'')^2(9a')^2(3a'')^2(10a').$$

The stationary point structures were completely optimized within the C_s symmetry constraints using analytic gradient techniques, until residual Cartesian coordinate gradients were less than 10^{-6} a.u. However, the cc-pVQZ/CCSD(T) gradients were determined using finite differences of energies while maintaining the 10^{-6} a.u. gradient convergence criterion. The self-consistent field (SCF) quadradic force constants were determined via analytic second derivatives, while the CCSD and CCSD(T) force constants were determined by finite differences of analytic gradients [DZP and TZ2P(f,d) basis sets] or finite differences of energies (cc-pVQZ basis set). Spin densities used to determine hyperfine splitting constants were computed at the CCSD and CCSD(T) levels utilizing the analytical coupled cluster relaxed density.[36–40] All computations were carried out using the PSI[41] and ACESII[42] program packages.

III. RESULTS

The optimized structures of H_2PO using ROHF and UHF wave functions are presented in Table I. As demonstrated by deWaal, Aagaard, and Janssen,[10] use of a ROHF wave function constructed within a small basis yields two minima of $^2A'$ symmetry which differ most notably in their P–O bond lengths. These can be thought of as resonance structures of the H_2PO radical, as the unpaired electron in the ''short'' P–O structure is localized on the phosphorus atom, while the single electron in the ''long'' P–O structure is described by an oxygen lone pair molecular orbital. Conversely, a UHF treatment yields only the long P–O oxygen-centered radical.

An illustrative comparison of the DZP/ROHF and UHF potential energy surfaces along the P–O coordinate is provided in Fig. 2. These curves were constructed by constrain-

TABLE I. Equilibrium bond lengths (Å) and bond angles (degrees) for H_2PO within the DZP and TZ2P(f,d) basis sets. Values using ROHF reference wave functions are given for both the ''short'' and ''long'' (in brackets) energy minima.

Basis set	Method	P–O		P–H		∠H–P–H		∠H–P–O	
DZP	ROHF	1.487	[1.636]	1.410	[1.412]	103.26	[96.71]	115.59	[100.69]
	ROHF-CCSD	1.534	[1.543]	1.422	[1.422]	101.77	[101.46]	113.53	[112.48]
	ROHF-CCSD(T)	1.539	[1.539]	1.425	[1.425]	101.55	[101.55]	113.76	[113.76]
	UHF	1.610		1.412		97.98		102.54	
	UHF-CCSD	1.537		1.422		101.67		113.14	
	UHF-CCSD(T)	1.538		1.425		101.57		113.76	
TZ2P(f,d)	ROHF	1.461	[1.597]	1.404	[1.406]	103.46	[97.34]	116.00	[102.08]
	ROHF-CCSD	1.494	[1.494]	1.407	[1.407]	102.66	[102.66]	114.67	[114.67]
	ROHF-CCSD(T)	1.503	[1.503]	1.411	[1.411]	102.37	[102.37]	114.49	[114.49]
	UHF	1.474		1.403		103.40		114.17	
	UHF-CCSD	1.497		1.407		102.59		114.31	
	UHF-CCSD(T)	1.501		1.411		102.44		114.73	
	Expt.[a]	1.4875(4)		1.4287(14)		102.56(14)		115.52(10)	

[a]Reference 9.

ing the P–O bond distance and optimizing all other geometrical parameters until the internal coordinate gradients were less than 10^{-6} a.u. This process was repeated at 0.001 Å intervals along the P–O coordinate. At the DZP/ROHF level, energy minima occur at $r(\mathrm{P–O})=1.487$ Å and $r(\mathrm{P–O})=1.636$ Å, a difference of 0.149 Å. The structures represented here fall along two different slices of the six-dimensional potential energy surface and appear to intersect only because they have been projected onto the P–O axis. Thus, the point of apparent intersection represents two distinct geometries—the primary differences lying in the H–P–O and H–P–H bond angles (103.26° vs 96.71° and 115.59° vs 100.69°, respectively). This difference in pyramidalization of the phosphorus further reflects the localization of the unpaired electron. Within the ''long'' P–O structure the unpaired electron resides on the oxygen leaving an electron pair on the phosphorus. This electron pair distorts the P–H bonds away from planarity more effectively than the single electron of the phosphorus-centered radical, providing a qualitative picture of the phosphorus hybridization at each energy minimum.

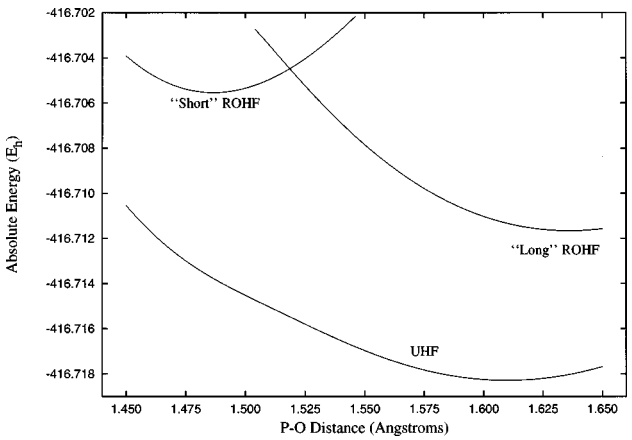

FIG. 2. Comparison of the DZP ROHF and UHF potential energy curves along the P–O coordinate. The ROHF formalism creates an artifactual double minimum surface while the UHF treatment shows a shoulder at a P–O distance near that of the short ROHF minimum.

The DZP/UHF curve shows a single minimum at a P–O distance of 1.610 Å. However, there is an interesting change in curvature along the DZP/UHF potential energy surface near the P–O bond length of the short DZP/ROHF minimum. Although not represented in the potential energy surface diagrams, curves constructed at the TZ2P (f,d)/ROHF level also reveal two minima at $r(\mathrm{P–O})=1.461$ Å and $r(\mathrm{P–O})=1.597$ Å, but the lower-energy structure swaps from the long to the short P–O bond geometry, placing the latter approximately 4 kcal/mol lower in energy. This result illustrates the near degeneracy of the $10a'$ and $11a'$ molecular orbitals and the apparent need for substantial inclusion of dynamical correlation as well as the potential importance of a multireference treatment.

As the level of theory is improved to DZP/ROHF-CCSD, the occurrence of the double minimum persists, but the energy difference between the minima is reduced and the similarity in geometries is greatly increased relative to the DZP/ROHF level. The short and long P–O bond lengths with the DZP/ROHF-CCSD method differ by only 0.009 Å, while the energy difference is less than 1 kcal/mol. It should also be noted that ROHF-based calculations at the TZ2P(f,d)/CCSD level predict only one minimum-energy structure at $r(\mathrm{P–O})=1.494$ Å, illustrating that the artifactual double minimum is also affected by increases in basis set size. UHF-reference treatments at the DZP/CCSD level again predict a single minimum energy structure. Similarly, within the DZP basis, Brueckner-orbital-based CCD[43,44] and quasi-restricted Hartree–Fock reference-based CCSD[32,44] treatments yield a single energy minimum. Within the DZP basis there is also a profound shortening of the P–O bond length from 1.610 to 1.537 Å as correlation is included moving from UHF to UHF-CCSD. This generally unexpected trend has also been reported by Nguyen and Ha,[16] who observed a shortening of the P–O bond length comparing UHF and UMP2 optimized structures. Artifactual minima can also be avoided by improving the degree of dynamical correlation and is observed even at the DZP/ROHF-CCSD(T) level as the curves converge to a single minimum at a P–O distance of 1.539 Å. This value, which is also in excellent agreement

TABLE II. Harmonic vibrational frequencies (cm^{-1}) for H_2PO within the DZP and TZ2P(f,d) basis sets. Values using ROHF reference wave functions are given for both the ''short'' and ''long'' (in brackets) energy minima.

Basis set	Method	a' P–H str	a' P–O str	a' H–P–H bend	a' H–P–O bend	a'' P–H str	a'' H–P–O bend
DZP	ROHF	2525 [2540]	1260 [779]	1201 [1238]	882 [973]	2552 [2540]	895 [917]
	ROHF-CCSD	2402 [2405]	1066 [1243]	1156 [1148]	664 [894]	2439 [2438]	839 [842]
	ROHF-CCSD(T)	2369 [2369]	1081 [1081]	1150 [1150]	805 [805]	2407 [2407]	824 [824]
	UHF	2532	647	1228	980	2540	932
	UHF-CCSD	2403	1062	1156	723	2438	840
	UHF-CCSD(T)	2371	1064	1148	725	2410	825
TZ2P(f,d)	ROHF	2520 [2532]	1338 [742]	1208 [1240]	946 [989]	2548 [2534]	910 [923]
	ROHF-CCSD	2414 [2414]	1197 [1197]	1140 [1140]	803 [803]	2457 [2457]	853 [853]
	ROHF-CCSD(T)	2380 [2380]	1167 [1167]	1118 [1118]	785 [785]	2427 [2427]	840 [840]
	UHF	2521	1235	1198	789	2553	917
	UHF-CCSD	2415	1179	1135	782	2458	855
	UHF-CCSD(T)	2382	1184	1127	804	2428	837
	Expt.[a]	2275	1147		833		791

[a]Reference 15.

with the DZP/UHF-CCSD(T) treatment, is an intermediate value characteristic of neither the short nor the long P–O bond lengths obtained at lower levels of theory.

Harmonic vibrational frequencies of H_2PO using the ROHF- and UHF-reference methods are compared in Table II. Of particular interest is the a' P–O stretch which has DZP/ROHF values of 1260 and 779 cm^{-1} for the ''short'' and ''long'' P–O structures, respectively. Naturally, the convergence of the P–O stretch parallels the convergence of the geometrical structure, and it is not until the TZ2P(f,d)/CCSD(T) level that one obtains good agreement with experiment for this mode. Certainly any prediction of the symmetric P–O stretching frequency directly depends upon the crucial P–O bond length and our illustrations supplement the work of deWaal *et al.*[10] in showing why values both higher and dramatically lower than the experimental value have been advanced in the literature.

In light of the sensitivity of the H_2PO structure to variations in basis set and electron correlation, an ambitious effort was made to extend the one particle basis to quadruple-ζ quality while maintaining the CCSD(T) level of theory. As shown in Table III the cc-pVQZ/UHF-CCSD(T) optimized structural parameters are in excellent agreement with the gas-phase microwave spectrum values, with the exception of the P–H distance which is surprisingly mediocre. The experimental P–H bond length is nearly 0.02 Å longer than the cc-pVQZ/UHF-CCSD(T) value which perhaps would lengthen slightly upon inclusion of the full triple excitations. Although the experimental substitution structure r_s is inherently different from the theoretical equilibrium geometry r_e, a difference of 0.02 Å in the P–H distance seems unlikely. The critical P–O bond distance, however, differs from experiment by only 0.005 Å. The totally symmetric harmonic vibrational frequencies were also determined at the cc-pVQZ/UHF-CCSD(T) level, and the comparison of these theoretical harmonic frequencies with the available experimental fundamental frequencies is presented in Table III. In particular, the cc-pVQZ/UHF-CCSD(T) P–O harmonic stretching frequency lies within 43 cm^{-1} of the experimental fundamental, clearly solidifying the original experimental assignment of this band by Withnall and Andrews.

TABLE III. Equilibrium bond lengths (Å), bond angles (degree), and totally symmetric harmonic vibrational frequencies (cm^{-1}) for H_2PO at the cc-pVQZ/UHF-CCSD(T) level of theory.

	P–O	P–H	∠H–P–H	∠H–P–O
cc-pVQZ/CCSD(T)	1.492	1.410	102.63	114.92
Expt.[a]	1.4875	1.4287	102.56	115.52
	P–H stretch	P–O stretch	H–P–H bend	H–P–O bend
cc-pVQZ/CCSD(T)	2366.5	1189.7	1122.4	813.0
Expt.[b]	2275	1147	⋯	833

[a]Reference 9.
[b]Reference 15.

With an accurate *ab initio* description of the phosphoryl bond, the hyperfine splitting (hfs) constants were determined for the ^{31}P, ^{1}H, and ^{17}O nuclei. The Fermi contact terms (a_F) for ^{1}H and ^{17}O as well as a_F and the anisotropic T_{ZZ} components of the hfs for the ^{31}P nucleus are compiled in Table IV and compared with those determined in previous studies. The relative magnitudes of the Fermi contact terms quantitatively reflect the unpaired spin density at each nucleus,[45] and the 6-31G*/ROHF a_F (^{31}P) values obtained by deWaal *et al.*[10] again illustrate the localization of the unpaired electron. The ^{31}P Fermi contact term of the ''short'' phosphorus-centered minimum is 942 MHz while that of the ''long'' oxygen-centered minimum is only 135 MHz, the latter in clear disagreement with the experimental value of 1023.43 MHz. Although density functional treatments using the B3LYP functional produce a reasonable value of 944.7 MHz,[18] a variety of other methods[10,16,17] have produced scattered results for a_F (^{31}P). In particular, the large structural change between the 6-311G**/UHF and 6-311G**/UMP2 levels results in a value of a_F (^{31}P) which more than doubles.

On the other hand, the TZ2P(f,d)/UHF-CCSD(T) values in Table IV are in very good agreement with experiment for both the isotropic and anisotropic components of the hyperfine splittings. The a_F (^{17}O) component may be com-

TABLE IV. Fermi contact terms (a_F) and anisotropic T_{ZZ} components (in MHz) of the hyperfine constants of ^{31}P, ^{1}H, and ^{17}O nuclei in H_2PO.

Method	$a_F(^{31}P)$	$T_{ZZ}(^{31}P)$	$a_F(^{1}H)$	$a_F(^{17}O)$
6-31G*/ROHF (short)[a]	942	333	⋯	−5
6-31G*/ROHF (long)[a]	135	34	⋯	0
6-311G**/UHF[b]	578.9	⋯	104.4	⋯
6-311G**/UMP2[b]	1278	⋯	81.0	⋯
DZP/CISD//6-31G**/UMP2[c]	859.1	⋯	75.9	⋯
TZVP″/B3LYP//6-311G(d,p)/B3LYP[d]	944.7	⋯	⋯	⋯
cc-pVQZ/UHF-CCSD(T)[e]	908.8	294.7	94.2	−19.8
TZ2P(f,d)/ROHF-CCSD(T)[e]	969.4	284.6	90.7	−27.9
TZ2P(f,d)/UHF-CCSD(T)[e]	995.7	290.1	90.9	−25.8
Expt. (H_2PO)[f]	1023.43	332.9	109.27	⋯
Expt. (Ar_2PO)[g]	1040	⋯	⋯	−26

[a]Reference 10.
[b]Reference 17.
[c]Reference 16.
[d]Reference 18.
[e]This work.
[f]Reference 9.
[g]Ar=2,4,6-tri-*tert*-butylphenyl. References 13 and 14.

pared with that of an aryl derivative[13,14] of H_2PO for which there are experimental data (see below). The TZ2P(f,d)/UHF-CCSD(T) values of a_F (^{31}P) and a_F (^{1}H) are 998.7 and 90.9 MHz, respectively—an average deviation of only 23 MHz from experiment. The Fermi contact term for ^{1}H and the T_{ZZ} component of the ^{31}P hfs are improved slightly at the cc-pVQZ/UHF-CCSD(T) level, however, the value of a_F (^{31}P) drops disappointingly to 908.8 MHz. This is consistent with the findings of Gauld, Eriksson, and Radom[46] who have shown in a systematic study that the cc-pVXZ and aug-cc-pVXZ basis sets display somewhat erratic fluctuations in hfs constants even at the cc-pVQZ level. Gauld and co-workers also note that large standard Pople basis sets such as 6-311+G($2df,p$) generally provide good results for isotropic splittings. The accuracy of the UHF-CCSD(T) hfs constants of this work using a similar tight *s*- and *p*-space TZ2P(f,d) basis support this trend.

IV. CONCLUSIONS

A definitive *ab initio* cc-pVQZ/CCSD(T) level prediction of the structure of the H_2PO radical has been obtained which compares well with the recent gas-phase microwave structure of Hirao, Saito, and Ozeki, with the exception of the P–H bond distance. In addition, the harmonic vibrational frequency corresponding to the P–O stretch was determined at this same level to be 1190 cm^{-1}, in close agreement with the experimental fundamental vibrational frequency of 1147 cm^{-1} obtained by Withnall and Andrews, thus solidifying the assignment of that spectral band. The intermediate values of the cc-pVQZ/CCSD(T) P–O vibrational frequency and bond length relative to those corresponding to the two artifactual ROHF minima are in accord with the experimental evidence of a highly delocalized unpaired electron. Although the hyperfine splitting constants of this radical were shown to be very sensitive to changes in basis set and level of theory, values determined at the TZ2P(f,d)/UHF-CCSD(T) level are in good agreement with available experimental data.

ACKNOWLEDGMENTS

This research was supported by the U.S. National Science Foundation, Grant No. CHE-9527468. S.S.W. was supported by a Department of Defense Graduate Fellowship and a Robert S. Mulliken Graduate Fellowship. E.M.J. was supported by a 1997 CCQC Summer Undergraduate Fellowship. M.L.L. was supported by a Samuel Francis Boys Graduate Fellowship. The authors wish to thank Dr. Ajith Perera, Dr. Wesley D. Allen, and Professor John F. Stanton for insightful discussions concerning this research.

[1] M. Jacobi and A. Henne, J. Radiat. Curing **10**, 16 (1983).
[2] M. Jacobi and A. Henne, Polym. Paint Color J. **175**, 636 (1985).
[3] W. Rutsch, K. Dietliker, D. Leppard, M. Kohler, L. Misev, U. Kolczak, and G. Rist, Prog. Organic Coatings **27**, 227 (1996).
[4] T. Sumiyoshi, W. Schnabel, A. Henne, and P. Lechtken, Polymer **26**, 141 (1985).
[5] T. Sumiyoshi and W. Schnabel, Makromol. Chem. **186**, 1811 (1985).
[6] A. Kajiwara, Y. Konishi, Y. Morishima, W. Schnabel, K. Kuwata, and M. Kamachi, Macromolecules **26**, 1656 (1993).
[7] M. Kamachi, A. Kajiwara, K. Saegusa, and Y. Morishima, Macromolecules **26**, 7369 (1993).
[8] U. Kolczak, G. Rist, K. Dietliker, and J. Wirz, J. Am. Chem. Soc. **118**, 6477 (1996).
[9] T. Hirao, S. Saito, and H. Ozeki, J. Chem. Phys. **105**, 3450 (1996).
[10] B. F. M. de Waal, O. M. Aagaard, and R. A. J. Janssen, J. Am. Chem. Soc. **113**, 9471 (1991).
[11] Y. Ayant, A. Therand, L. Werbelov, and P. Tordo, J. Magn. Reson. **72**, 251 (1987).
[12] G. Sluggett, P. McGarry, I. Koptyug, and N. Turro, J. Am. Chem. Soc. **118**, 7367 (1996).
[13] N. J. Winter, J. Fossey, B. Beccard, Y. Berchadsky, F. Vila, L. Werbelow, and P. Tordo, J. Phys. Chem. **90**, 6749 (1986).
[14] Y. Ayant, A. Thevand, L. Werbelow, and P. Tordo, J. Magn. Reson. **72**, 251 (1987).
[15] R. Withnall and L. Andrews, J. Phys. Chem. **92**, 4610 (1988).
[16] M. T. Nguyen and T. K. Ha, Chem. Phys. **131**, 245 (1989).

[17] C. J. Cramer and M. H. Lim, J. Phys. Chem. **98**, 5024 (1994).
[18] M. Nguyen, S. Creve, and L. Vanquickenborne, J. Phys. Chem. **101**, 3174 (1997).
[19] S. Yabushita and M. S. Gordon, Chem. Phys. Lett. **91**, 1743 (1987).
[20] J. A. Boatz, M. W. Schmidt, and M. S. Gordon, J. Phys. Chem. **91**, 1743 (1987).
[21] K. E. Edgecombe, J. Mol. Struct.: THEOCHEM **226**, 157 (1991).
[22] S. Huzinaga, J. Chem. Phys. **42**, 1293 (1965).
[23] T. H. Dunning, J. Chem. Phys. **53**, 2823 (1970).
[24] T. H. Dunning and P. J. Hay, in *Modern Theoretical Chemistry*, edited by H. F. Schaefer (Plenum, New York, 1977), Vol. 3, p. 1.
[25] T. H. Dunning, J. Chem. Phys. **90**, 1007 (1989).
[26] D. E. Woon and T. H. Dunning, J. Chem. Phys. **98**, 1358 (1993).
[27] A. D. McLean and G. Chandler, J. Chem. Phys. **72**, 5639 (1980).
[28] T. H. Dunning, J. Chem. Phys. **55**, 716 (1971).
[29] $\alpha_f(\mathrm{P}) = 0.452$; $\alpha_f(\mathrm{O}) = 1.428$.
[30] $\alpha_d(\mathrm{H}) = 1.057$.
[31] G. D. Purvis and R. J. Bartlett, J. Chem. Phys. **76**, 1910 (1982).
[32] M. Rittby and R. J. Bartlett, J. Phys. Chem. **92**, 3033 (1988).
[33] K. Raghavachari, G. W. Trucks, J. A. Pople, and M. Head-Gordon, Chem. Phys. Lett. **157**, 479 (1989).
[34] R. J. Bartlett, J. D. Watts, S. A. Kucharski, and J. Noga, Chem. Phys. Lett. **165**, 513 (1990), erratum: **167**, 609 (1990).
[35] J. Gauss, W. J. Lauderdale, J. F. Stanton, J. D. Watts, and R. J. Bartlett, Chem. Phys. Lett. **182**, 207 (1991).
[36] J. Gauss, J. F. Stanton, and R. J. Bartlett, J. Chem. Phys. **95**, 2639 (1991).
[37] J. Gauss, W. J. Lauderdale, J. F. Stanton, J. D. Watts, and R. J. Bartlett, Chem. Phys. Lett. **182**, 207 (1991).
[38] J. D. Watts, J. Gauss, and R. J. Bartlett, Chem. Phys. Lett. **200**, 1 (1992).
[39] J. D. Watts, J. Gauss, and R. J. Bartlett, J. Chem. Phys. **98**, 8718 (1993).
[40] S. A. Perera, J. D. Watts, and R. J. Bartlett, J. Chem. Phys. **100**, 1425 (1994).
[41] C. L. Janssen, E. T. Seidl, G. E. Scuseria, T. P. Hamilton, Y. Yamaguchi, R. B. Remington, Y. Xie, G. Vacek, C. D. Sherrill, T. D. Crawford, J. T. Fermann, W. D. Allen, B. R. Brooks, G. B. Fitzgerald, D. J. Fox, J. F. Gaw, N. C. Handy, W. D. Laidig, T. J. Lee, R. M. Pitzer, J. E. Rice, P. Saxe, A. C. Scheiner, and H. F. Schaefer, PSI 2.0.8, PSITECH, Inc., Watkinsville, GA 30677, 1995. This program is generally available for a handling fee of $100.
[42] J. F. Stanton, J. Gauss, W. J. Lauderdale, J. D. Watts, and R. J. Bartlett, ACES II. The package also contains modified versions of the MOLECULE Gaussian integral program of J. Almlöf and P. R. Taylor, the ABACUS integral derivative program written by T. U. Helgaker, H. J. Aa. Jensen, P. Jørgensen, and P. R. Taylor, and the PROPS property evaluation integral code of P. R. Taylor.
[43] N. C. Handy, J. A. Pople, M. Head-Gordon, K. Raghavachari, and G. W. Trucks, Chem. Phys. Lett. **164**, 185 (1989).
[44] J. F. Stanton, J. Gauss, and R. J. Bartlett, J. Chem. Phys. **97**, 5554 (1992).
[45] W. Weltner, *Magnetic Atoms and Molecules* (Van Nostrand, New York, 1983).
[46] J. W. Gauld, L. A. Eriksson, and L. Radom, J. Phys. Chem. **101**, 1352 (1997).